

# Inverse Dynamics Analysis of a 6-PSS Parallel Manipulator

Weiyuan Xu<sup>1</sup>, Yangmin Li<sup>1,2,\*</sup>, Song Lu<sup>1</sup>, and Xiao Xiao<sup>1</sup>

<sup>1</sup> Department of Electromechanical Engineering, University of Macau,  
Avenida da Universidade, Taipa, Macao SAR, China

yml@umac.mo

<sup>2</sup> Tianjin Key Laboratory of the Design and Intelligent Control of the Advanced  
Mechatronics System, Tianjin University of Technology, Tianjin 300384, China

**Abstract.** In this paper, a new six degrees of freedom (6-DOF) parallel manipulator with adjustable actuators is proposed. The kinematic model is firstly established and the kinematic analysis is performed afterward. Then the equations of motion are developed based on the concept of link Jacobian matrices. Finally, the principle of virtual work is applied to analyze the dynamics of this 6-PSS parallel manipulator. This methodology can be used on other types of parallel manipulators not only for 6-DOF but also with less than 6-DOF. To solve the inverse dynamics of the manipulator, a computational algorithm is developed and two trajectories of the moving platform are simulated.

**Keywords:** 6-PSS parallel manipulator, Kinematics, Dynamics, Virtual work.

## 1 Introduction

In the last decades, although the serial manipulators have been widely used in the industrial fields, the requirement for more efficient on the robotic operation is still increasing, which drives the engineers to design some typical parallel robots, such as Giddings & Lewis, Ingersoll and Hexel or even some micro parallel manipulators for the high precision application [1]. A parallel manipulator mostly consists of three parts: a moving platform, a fixed base and several limbs that connect the platform and the base. Because the actuators can be mounted on the fixed base of the manipulator, the weights of the moving components (limbs and moving platform) can be reduced, which will minimize the effect of the inertia of the limbs on the operation. Therefore, the parallel manipulator has some inherent advantages than traditional serial manipulator, such as: higher positioning accuracy, better rigidity and larger load capacity.

It is meaningful to develop the dynamical model of the robot because the dynamical analysis is essential for the computer simulation, control strategy development and physical prototype optimization [2]-[3]. Typically, there are two

---

\* Corresponding author.

problems for the dynamics analysis of parallel manipulator: forward and inverse dynamics [4]. The forward dynamics is about a situation that the input forces or the moments are given and we will calculate the position and orientation of the moving platform. On the other hand, the inverse dynamics is to gain the input forces or moments of the actuators with respect to the given motion trajectories of the moving platform. And this model later can be used to design the dynamic controller. Over the last three decades, several researchers have made contributions to the dynamic analysis of parallel manipulator. Some typical approaches that have been proposed include the Newton-Euler formulation [5]-[7], the Lagrangian formulation [8]-[10] and the principle of virtual work [2], [4], [11]. Other new approaches also have been studied such as the Kane method [12]-[14].

Because the kinematic model of the spatial parallel manipulator is complex, it is very normal to make some assumptions to simplify the expressions of the kinetic and potential energy when applying the Newton-Euler or Lagrangian methods [15]-[16]. Therefore, these approaches sometimes are not accurate and efficient enough for the dynamic analysis of parallel manipulator on some perspective. In this paper, we select the principle of virtual work to develop the dynamic modeling of this 6-PSS parallel manipulator. The method presented in this paper is similar to that used in Tsai [2] and Gosselin [11]. However, the process for developing the Jacobian matrices is different from that of [2], which makes it more easier and normal to form the motion equations. Moreover, this method is also suitable for other closed-loop structures dynamic analysis, such as other types of parallel manipulators.

In what follows, the structure of this 6-PSS parallel manipulator is illustrated with a three dimensional model. Then, the inverse kinematics are analyzed and a new method to define the link Jacobian is proposed. Thirdly, the dynamic equations of motion are formulated based on the principle of virtual work. Finally, a computational algorithm is developed to solve the inverse dynamic equations by MATLAB software and some simulations are made with respect to two given trajectories.

## 2 Kinematic Analysis

### 2.1 Illustration of the 6-PSS Parallel Manipulator

The architecture of the 6-PSS parallel mechanism is shown in Fig.1 that is composed of a fixed base, a moving platform, three triangle rail trusses and six identical limbs. The details of this manipulator has been described in [17].

As shown in Fig.1, the 3D prototype of the 6-PSS parallel manipulator, there are 14 links connected by 6 prismatic joints and 12 spherical joints. Hence, the number of the degrees of freedom of such mechanism is

$$F = \lambda(n - j - 1) + \sum_i f_i = 6(14 - 18 - 1) + (6 + 3 \times 12) = 12 \quad (1)$$

However, there are 6 passive degrees of freedom associated with these six PSS limbs. Therefore, the moving platform possesses 6 degrees of freedom.

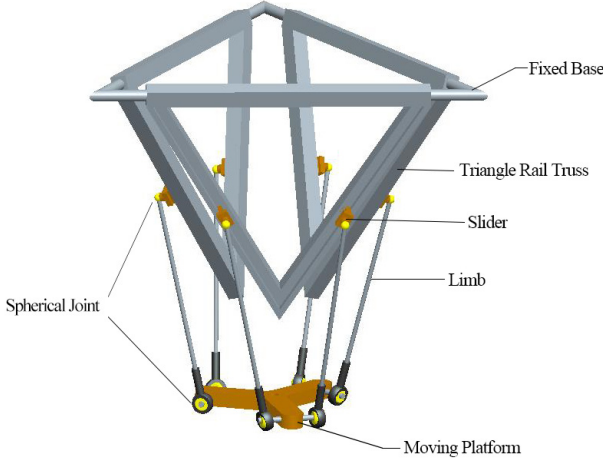


**Fig. 1.** A 3D prototype of the 6-PSS parallel manipulator

## 2.2 Kinematics Model

For the purpose of kinematic analysis, two Cartesian coordinate systems  $O(x, y, z)$  and  $B(u, v, w)$  are attached to the fixed base and the moving platform, respectively. As shown in Fig. 2, the  $O(x, y, z)$  frame is attached at the center point  $O$  of the fixed congruent triangle base platform  $\Delta M_1M_2M_3$  ( $M_1, M_2, M_3$  are the cross sectional points of the central lines of the sides.). And the  $B(u, v, w)$  frame is attached on the moving platform at point  $P$  that is the center of the hexagon  $B_1B_2B_3B_4B_5B_6$ , which indicates the origin of frame  $B(u, v, w)$  coincides with the center point  $P$ . The  $x$ -axis is along the direction of vector  $M_2O$ , and the  $y$ -axis is parallel to vector  $C_5C_6$ . And for the frame  $B(u, v, w)$ , the  $u$ -axis is perpendicular to the line  $B_5B_6$ , same direction with  $x$ -axis and the  $v$ -axis is alongside the  $y$ -axis on origin. Both the  $z$ -axis and  $\omega$ -axis are defined by the right-hand rule.

In this study, we assume that  $OM_k = R$  ( $k = 1, 2, 3$ ),  $BB_i = r$ ,  $C_iD_i = L$  and  $A_iB_i = l$ . The angle  $\varphi$  between planes  $C_1C_2D_1$  and  $C_1C_2C_4$  is defined as the angle layout of actuator, and  $\theta$  is for the angle between  $PB_2$  and the mid-perpendicular line of line segment  $B_1B_2$ .

The coordinates transformation of the moving points  $B_i$  from the moving frame  $B(u, v, w)$  to the fixed frame  $O(x, y, z)$  can be described by the position vector  $\mathbf{p} = [p_x \ p_y \ p_z]^T$  of the centroid  $P$  and the rotation matrix  ${}^O R_B$  in a  $[3 \times 3]$  matrix. Let  $\mathbf{u}, \mathbf{v}$  and  $\mathbf{w}$  be the three unit vectors defined along with  $u, v$  and  $w$  axes of the frame  $B(u, v, w)$ , and the  ${}^O R_B$  can be defined as a rotation of  $\gamma$  about the fixed  $x$ -axis, followed by a rotation of  $\beta$  about the fixed  $y$ -axis, and a rotation of  $\alpha$  about the fixed  $z$ -axis, thus it yields  ${}^O R_B$  to

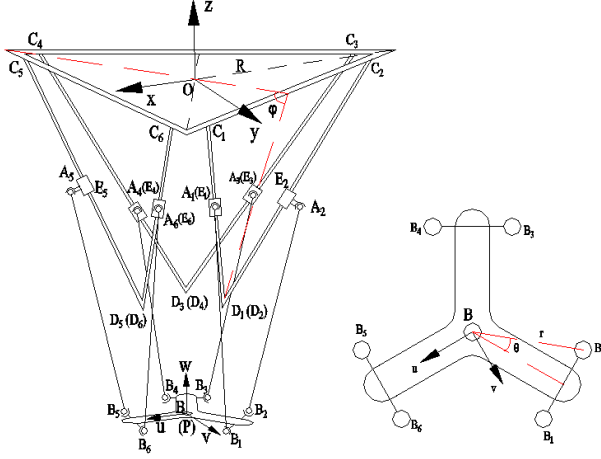


Fig. 2. Schematic representation of the 6-PSS parallel manipulator

$$\begin{aligned}
 {}^O R_B &= R_X(\gamma)R_Y(\beta)R_Z(\alpha) \\
 &= \begin{bmatrix} c\alpha c\beta & c\alpha s\beta s\gamma - s\alpha c\gamma & c\alpha s\beta c\gamma + s\alpha s\beta \\ s\alpha c\beta & -s\alpha s\beta s\gamma + c\alpha c\gamma & -s\alpha s\beta c\gamma - c\alpha c\gamma \\ -s\beta & c\beta s\gamma & c\beta c\gamma \end{bmatrix}. \quad (2)
 \end{aligned}$$

According to the structure of the model in Fig.2, the coordinates of the points  $B_i$  on the moving platform can be obtained with reference to the fixed frame  $O$  by using a closed-loop vector as follows:

$$OC_i + d_i \mathbf{s}_i + E_i A_i + l \mathbf{k}_i = \mathbf{p} + \mathbf{b}_i. \quad (3)$$

where

$d_i$  is the displacement of corresponding slider  $E_i$ ;

$\mathbf{k}_i$  is the unit vector of limb  $i$  with respect to fixed frame  $O$ ;

$\mathbf{b}_i = {}^O R_B {}^B \mathbf{b}_i$  and  ${}^B \mathbf{b}_i$  are the coordinates of  $B_i$  with respect to frame  $B$ ;

$\mathbf{s}_i$  is the unit vector of the groove of the triangle truss  $i$ , respectively.

$$\mathbf{s}_i = \frac{C_i D_i}{L}. \quad (4)$$

Then by solving Eq.(3), we will find the vector  $\mathbf{k}_i$  by

$$\mathbf{k}_i = \frac{\mathbf{p} + \mathbf{b}_i - OC_i - d_i \mathbf{s}_i - E_i A_i}{l}. \quad (5)$$

## 2.3 Velocity Analysis

Before computing the motion equations of this manipulator, it is necessary to analyze the kinematic characteristics of each reference limb. According to the

definition of the position and rotation matrix of the moving platform, we have the linear and angular velocities of it as follows

$$\mathbf{V}_p = [\dot{p}_x \ \dot{p}_y \ \dot{p}_z]^T. \quad (6)$$

$$\boldsymbol{\omega}_p = [\dot{\gamma} \ \dot{\beta} \ \dot{\alpha}]^T. \quad (7)$$

The velocity of the center of a spherical joint  $B_i$  can be obtained by taking the derivative of the right-hand side of Eq.(3) with respect to time.

$$\mathbf{V}_{bi} = \mathbf{V}_p + \boldsymbol{\omega}_p \times \mathbf{b}_i. \quad (8)$$

Next, taking the derivative of the left-hand side of Eq.(3) with respect to time, we have another expression as follows:

$$\mathbf{V}_{bi} = \dot{d}_i \mathbf{s}_i + l \boldsymbol{\omega}_i \times \mathbf{k}_i. \quad (9)$$

Dot multiplying both sides of Eq.(9) with  $\mathbf{k}_i$  yields

$$\dot{d}_i = \frac{\mathbf{k}_i^T \cdot \mathbf{V}_{bi}}{\mathbf{k}_i^T \cdot \mathbf{s}_i}. \quad (10)$$

Cross multiplying both sides of Eq.(9) with  $\mathbf{k}_i$  yields to

$$\boldsymbol{\omega}_i = \frac{1}{l} \left[ \mathbf{k}_i \times \mathbf{V}_{bi} - \dot{d}_i \mathbf{k}_i \times \mathbf{s}_i \right]. \quad (11)$$

In this paper, we suppose that the center of mass of limb  $i$  is at the geometry center, then we have

$$\mathbf{C}_{mi} = \mathbf{O}C_i + d_i \mathbf{s}_i + E_i A_i + \frac{l}{2} \mathbf{k}_i. \quad (12)$$

Taking derivative of Eq.(12) with respect to time, we have the velocity of the center of mass of limb  $i$  as follows

$$\mathbf{V}_{li} = \dot{d}_i \mathbf{s}_i + \frac{l}{2} \boldsymbol{\omega}_i \times \mathbf{k}_i. \quad (13)$$

## 2.4 Acceleration Analysis

The acceleration items of the moving platform can be obtained by taking the secondary derivative of the corresponding items as follows

$$\dot{\mathbf{V}}_p = [\ddot{p}_x \ \ddot{p}_y \ \ddot{p}_z]^T. \quad (14)$$

$$\dot{\boldsymbol{\omega}}_p = [\ddot{\gamma} \ \ddot{\beta} \ \ddot{\alpha}]^T. \quad (15)$$

The acceleration of points  $B_i$  is obtained by taking the time derivative of Eq.(8).

$$\dot{\mathbf{V}}_{bi} = \dot{\mathbf{V}}_p + \dot{\boldsymbol{\omega}}_p \times \mathbf{b}_i + \boldsymbol{\omega}_p \times (\boldsymbol{\omega}_p \times \mathbf{b}_i). \quad (16)$$

By taking the derivative of Eq.(9) with respect to time, it yields another expression of the acceleration of point  $B_i$  as follows

$$\dot{\mathbf{V}}_{bi} = \ddot{d}_i \mathbf{s}_i + l \dot{\boldsymbol{\omega}}_i \times \mathbf{k}_i + l \boldsymbol{\omega}_i \times (\boldsymbol{\omega}_i \times \mathbf{k}_i). \quad (17)$$

Dot multiplying both sides of Eq.(17) with  $\mathbf{k}_i$  yields to

$$\ddot{d}_i = \frac{1}{\mathbf{k}_i^T \cdot \mathbf{s}_i} \left( \mathbf{k}_i^T \cdot \dot{\mathbf{V}}_{bi} + l \boldsymbol{\omega}_i^T \cdot \boldsymbol{\omega}_i \right). \quad (18)$$

To find the angular acceleration of limb  $i$ , we can cross multiply both sides of Eq.(17) with  $\mathbf{k}_i$ .

$$\dot{\boldsymbol{\omega}}_i = \frac{1}{l} \left[ \mathbf{k}_i \times \dot{\mathbf{V}}_{bi} - \frac{\mathbf{k}_i \times \mathbf{s}_i}{\mathbf{k}_i^T \cdot \mathbf{s}_i} \left( \mathbf{k}_i^T \cdot \dot{\mathbf{V}}_{bi} + l \boldsymbol{\omega}_i^T \cdot \boldsymbol{\omega}_i \right) \right]. \quad (19)$$

The acceleration of the centre of mass of limb  $i$  can be obtained by taking derivative of Eq.(13) with respect to time.

$$\dot{\mathbf{V}}_{li} = \ddot{d}_i \mathbf{s}_i + \frac{l}{2} [\dot{\boldsymbol{\omega}}_i \times \mathbf{k}_i + \boldsymbol{\omega}_i \times (\boldsymbol{\omega}_i \times \mathbf{k}_i)]. \quad (20)$$

### 3 Jacobian Matrices

#### 3.1 Jacobian Matrix of the Moving Platform

The Jacobian matrices are necessary for formulating the equations of motion, while the derivatives of the components are essential for formulating the corresponding Jacobian matrices. Writing Eq.(8) in matrix form yields to

$$\mathbf{V}_{bi} = J_{bi} \dot{\mathbf{X}}_p. \quad (21)$$

where  $\dot{\mathbf{X}}_p = [\mathbf{V}_p, \boldsymbol{\omega}_p]$  is a  $[6 \times 1]$  matrix representing the linear and angular velocities of the moving platform, and the Jacobian matrix  $J_{bi}$  is a  $[3 \times 6]$  matrix.

$$J_{bi} = \begin{bmatrix} 1 & 0 & 0 & 0 & b_{iz} & -b_{iy} \\ 0 & 1 & 0 & -b_{iz} & 0 & b_{ix} \\ 0 & 0 & 1 & b_{iy} & -b_{ix} & 0 \end{bmatrix}. \quad (22)$$

The Eq.(10) can be expressed in the form of  $y = ax$  as follows:

$$\dot{d}_i = J'_{inv-i} \mathbf{V}_{bi}. \quad (23)$$

where

$$J'_{inv-i} = \frac{\mathbf{k}_i^T}{\mathbf{k}_i^T \cdot \mathbf{s}_i}. \quad (24)$$

Substituting Eq.(21) (22) into Eq.(23) yields to

$$\dot{d}_i = J_{inv\_i} \dot{\mathbf{X}}_p, J_{inv\_i} = J'_{inv\_i} J_{bi}. \quad (25)$$

Rewriting the Eq.(25) for six times, we will find the inverse Jacobian matrix of the six actuators as follows

$$\dot{\mathbf{d}} = J_{inv} \dot{\mathbf{X}}_p. \quad (26)$$

where

$$J_{inv} = [J_{inv\_1} \cdots J_{inv\_6}]_{1 \times 6}^T. \quad (27)$$

### 3.2 Jacobian Matrix of the Sliders

According to the definition of  $\dot{d}_i$ , it can be seen that the value of the velocity of slider  $i$  is equal to  $\dot{d}_i$ .

$$\mathbf{V}_{si} = \dot{d}_i \mathbf{s}_i. \quad (28)$$

Substituting Eq. (25) into Eq.(28), we have

$$\mathbf{V}_{si} = J_{sVi} \dot{\mathbf{X}}_p. \quad (29)$$

where

$$J_{sVi} = [s_{ix} J_{inv\_i} \ s_{iy} J_{inv\_i} \ s_{iz} J_{inv\_i}]_{1 \times 3}^T. \quad (30)$$

Since the slider is constrained in the groove of the triangle truss, there is no rotation of the slider, i.e.  $\omega_{si} = 0$ . Therefore, we can deduct the Jacobian matrix of the slider  $i$  as follows:

$$\dot{\mathbf{X}}_{si} = J_{si} \dot{\mathbf{X}}_p, J_{si} = \begin{bmatrix} J_{sVi} \\ \mathbf{0}_{3 \times 6} \end{bmatrix}. \quad (31)$$

### 3.3 Jacobian Matrix of the Limbs

To find the Jacobian matrix of the limb  $i$ , we have to do some transformations on Eq. (13). Substituting Eq. (8), (10) and (11) into Eq.(13) yields to

$$\mathbf{V}_{li} = \mathbf{E}_i \cdot \mathbf{V}_{bi} \cdot \mathbf{F}_i + \frac{1}{2} \mathbf{k}_i \times \mathbf{V}_{bi} \times \mathbf{k}_i. \quad (32)$$

where

$$\mathbf{E}_i = J'_{inv\_i}, \mathbf{F}_i = \mathbf{s}_i - \frac{1}{2} \mathbf{k}_i \times \mathbf{s}_i \times \mathbf{k}_i. \quad (33)$$

By developing the vector  $\mathbf{E}_i = [E_{ix} \ E_{iy} \ E_{iz}]^T$ ,  $\mathbf{F}_i = [F_{ix} \ F_{iy} \ F_{iz}]^T$ ,  $\mathbf{k}_i = [k_{ix} \ k_{iy} \ k_{iz}]^T$ , we can obtain the Jacobian matrix of linear velocity of limb  $i$  as follows

$$\mathbf{V}_{li} = J_{lVi} \mathbf{V}_{bi}. \quad (34)$$

where

$$J_{IVi} = J_{IV1-i} + J_{IV2-i}. \quad (35)$$

$$J_{IV1-i} = \begin{bmatrix} E_{ix}F_{ix} & E_{iy}F_{ix} & E_{iz}F_{ix} \\ E_{ix}F_{iy} & E_{iy}F_{iy} & E_{iz}F_{iy} \\ E_{ix}F_{iz} & E_{iy}F_{iz} & E_{iz}F_{iz} \end{bmatrix}. \quad (36)$$

$$J_{IV2-i} = \begin{bmatrix} k_{iy}^2 + k_{iz}^2 & -k_{ix}k_{iy} & -k_{ix}k_{iz} \\ -k_{ix}k_{iy} & k_{ix}^2 + k_{iz}^2 & -k_{iy}k_{iz} \\ -k_{ix}k_{iz} & -k_{iy}k_{iz} & k_{ix}^2 + k_{iy}^2 \end{bmatrix}. \quad (37)$$

Similarly, we can find the Jacobian matrix of angular velocity of limb  $i$  based on Eq. (10) and (11).

$$\boldsymbol{\omega}_i = \frac{1}{l} \left[ \mathbf{k}_i \times \mathbf{V}_{bi} - \frac{\mathbf{k}_i \times \mathbf{s}_i}{\mathbf{k}_i^T \cdot \mathbf{s}_i} (\mathbf{k}_i^T \cdot \mathbf{V}_{bi}) \right] = \frac{1}{l} [\mathbf{k}_i \times \mathbf{V}_{bi} - \mathbf{Q}_i (\mathbf{k}_i^T \cdot \mathbf{V}_{bi})]. \quad (38)$$

where

$$\mathbf{Q}_i = \frac{\mathbf{k}_i \times \mathbf{s}_i}{\mathbf{k}_i^T \cdot \mathbf{s}_i} = [Q_{ix} \ Q_{iy} \ Q_{iz}]^T. \quad (39)$$

The two terms of Eq.(38) are as follows:

$$\mathbf{k}_i \times \mathbf{V}_{bi} = \begin{bmatrix} k_{iy}V_{biz} - k_{iz}V_{biy} \\ k_{iz}V_{bix} - k_{ix}V_{biz} \\ k_{ix}V_{biy} - k_{iy}V_{bix} \end{bmatrix}. \quad (40)$$

$$\mathbf{k}_i^T \cdot \mathbf{V}_{bi} = k_{ix}V_{bix} + k_{iy}V_{biy} + k_{iz}V_{biz}. \quad (41)$$

Substitute Eq.(39-41) into Eq.(38), it yields the angular velocity Jacobian matrix as follows

$$\boldsymbol{\omega}_i = J_{I\omega i} \mathbf{V}_{bi}. \quad (42)$$

where

$$J_{I\omega i} = \frac{1}{l} \begin{bmatrix} -k_{ix}Q_{ix} & -k_{iz} - k_{iy}Q_{ix} & k_{iy} - k_{iz}Q_{ix} \\ k_{iz} - k_{ix}Q_{iy} & -k_{iy}Q_{ix} & -k_{ix} - k_{iz}Q_{iy} \\ -k_{iy} - k_{ix}Q_{iz} & k_{ix} - k_{iy}Q_{iz} & -k_{iz}Q_{iz} \end{bmatrix}. \quad (43)$$

Therefore, the equation of motion of the limb  $i$  can be expressed as

$$\dot{\mathbf{X}}_{li} = \begin{bmatrix} \mathbf{V}_{li} \\ \boldsymbol{\omega}_{li} \end{bmatrix}. \quad (44)$$

By substituting Eq.(21), (34), (42) into Eq.(44), we get the Jacobian matrix of the limb  $i$  as follows

$$\dot{\mathbf{X}}_{li} = J_{li} \dot{\mathbf{X}}_p, J_{li} = \begin{bmatrix} J_{lvi} \\ J_{I\omega i} \end{bmatrix} J_{bi}. \quad (45)$$



## 4 Virtual Work

### 4.1 Applied and Inertia Wrenches

The resultant of the applied and inertia forces exerted at the center of mass of the moving platform is

$$\mathbf{F}_p = \begin{bmatrix} \hat{\mathbf{f}}_p \\ \hat{\mathbf{n}}_p \end{bmatrix} = \begin{bmatrix} \mathbf{f}_e + m_p \mathbf{g} - m_p \dot{\mathbf{V}}_p \\ \mathbf{n}_e - {}^O \mathbf{I}_p \dot{\boldsymbol{\omega}}_p - \boldsymbol{\omega}_p \times ({}^O \mathbf{I}_p \boldsymbol{\omega}_p) \end{bmatrix}. \quad (46)$$

where  $\mathbf{f}_e$  and  $\mathbf{n}_e$  are the external force and moment exerted at the center of mass, and in this paper, we assume they are equal to zero. And  ${}^O \mathbf{I}_p$  is the inertia tensor of the moving platform taken about the center of mass and expressed in the fixed frame  $O$ .

In this paper, we assume that the external force exerted at the sliders and the limbs is only the gravitational force, and since there is no rotation for the slider  $i$ , i.e.  $\omega_{si} = 0$ ,  $\dot{\omega}_{si} = 0$ , then the resultants of applied and inertia forces exerted at the center of mass of the slider  $i$  can be expressed as following equation.

$$\mathbf{F}_{si} = \begin{bmatrix} \hat{\mathbf{f}}_{si} \\ \hat{\mathbf{n}}_{si} \end{bmatrix} = \begin{bmatrix} m_s \mathbf{g} - m_s \dot{\mathbf{V}}_{si} \\ 0 \end{bmatrix}. \quad (47)$$

In the Section 2 and 3, we have deducted the necessary items of the limbs, so it is straightforward to find the force and moment of limb  $i$ .

$$\mathbf{F}_{li} = \begin{bmatrix} \hat{\mathbf{f}}_{li} \\ \hat{\mathbf{n}}_{li} \end{bmatrix} = \begin{bmatrix} m_l \mathbf{g} - m_l \dot{\mathbf{V}}_{li} \\ -{}^O \mathbf{I}_{li} \dot{\boldsymbol{\omega}}_{li} - \boldsymbol{\omega}_{li} \times ({}^O \mathbf{I}_{li} \boldsymbol{\omega}_{li}) \end{bmatrix}. \quad (48)$$

### 4.2 Equations of Motion

In this section, the procedure for solving the inverse dynamics of this 6-PSS parallel manipulator is proposed. The principle of virtual work for implementation on this manipulator can be expressed as

$$\delta \mathbf{q}_s^T \boldsymbol{\tau} + \delta \mathbf{X}_p^T \mathbf{F}_p + \sum_1^6 \left( \delta \mathbf{X}_{si}^T \mathbf{F}_{si} + \delta \mathbf{X}_{li}^T \mathbf{F}_{li} \right) = 0. \quad (49)$$

The virtual displacements  $\delta \mathbf{q}_s$ ,  $\delta \mathbf{X}_{si}$ ,  $\delta \mathbf{X}_{li}$  in Eq.(49) should be compatible with the kinematic constraints imposed by the structure. Therefore, it is necessary to relate the above virtual displacements to a set of independent virtual displacements  $\delta \mathbf{X}_p$ . Based on the d'Alembert's principle, the virtual displacement is equal to the derivative of the displacement with respect to time, hence we have

$$\delta \mathbf{q}_s = J_{inv} \delta \mathbf{X}_p, \delta \mathbf{X}_{si} = J_{si} \delta \mathbf{X}_p, \delta \mathbf{X}_{li} = J_{li} \delta \mathbf{X}_p. \quad (50)$$

Substituting Eq.(50) into Eq.(49) yields to

$$\delta \mathbf{X}_p^T \left[ J_{inv}^T \boldsymbol{\tau} + \mathbf{F}_p + \sum_{i=1}^6 (J_{si}^T \mathbf{F}_{si} + J_{li}^T \mathbf{F}_{li}) \right] = 0. \quad (51)$$

Since Eq.(51) is valid for any values of  $\delta \mathbf{X}_p^T$ , the condition to satisfy it is

$$J_{inv}^T \boldsymbol{\tau} + \mathbf{F}_p + \sum_{i=1}^6 (J_{si}^T \mathbf{F}_{si} + J_{li}^T \mathbf{F}_{li}) = 0. \quad (52)$$

Equation (52) describes the dynamics of this 6-PSS parallel manipulator. Therefore, if  $J_{inv}$  is not singular, the input force of the six actuators can be determined by the solution of Eq.(52).

$$\boldsymbol{\tau} = -J_{inv}^{-T} \left[ \mathbf{F}_p + \sum_{i=1}^6 (J_{si}^T \mathbf{F}_{si} + J_{li}^T \mathbf{F}_{li}) \right]. \quad (53)$$

Because this analysis is based on the assumption of the inverse of the transpose of the manipulator Jacobian matrix, when the moving platform approaches a singular configuration, the computation of input forces may become numerically unstable.

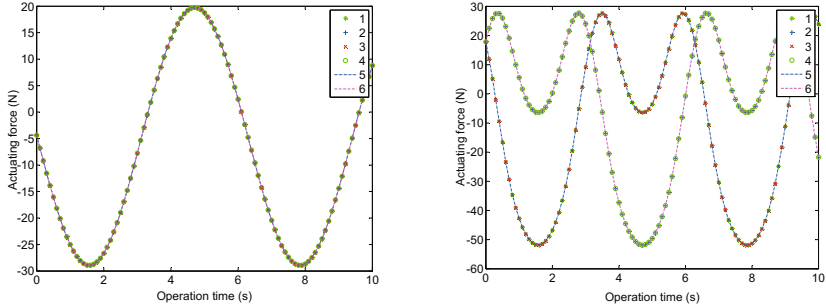
## 5 Numerical Simulation

In this section, a simulation is performed by the computer algorithm to verify this method. From the previous assumption, the external force acting on the items of the structure is only the gravitational force, and here, the gravity acceleration vector is  $\mathbf{g} = [0 \ 0 \ -9.807]^T m/s^2$ . Some values of the relevant parameters of this program are listed as:  $R = 400 \text{ mm}$ ,  $r = 120 \text{ mm}$ ,  $L = 450 \text{ mm}$ ,  $\varphi = 65^\circ$ ,  $\theta = 24.13^\circ$ , and the others can be found in [16]. The mass properties of the relevant components are obtained by the Solidworks simulation function:  $m_p = 829.3 \text{ g}$ ,  $m_l = 300.85 \text{ g}$ ,  $m_s = 73.93 \text{ g}$ . Based on the dimensions of the components, the inertia tensors can be developed as follows:

$${}^B I_p = \begin{bmatrix} 3.29 & 0 & 0 \\ 0 & 6.56 & 0 \\ 0 & 0 & 3.29 \end{bmatrix} \cdot 10^{-3} \text{ kg} \cdot \text{m}^2, \quad I_l = \begin{bmatrix} 0 & 0 & 0 \\ 0 & 2.04 & 0 \\ 0 & 0 & 2.04 \end{bmatrix} \cdot 10^{-2} \text{ kg} \cdot \text{m}^2$$

For the simulation, there are two scenarios to perform it. The first scenario is that the orientation of the moving platform remains constant while the center of mass of it moves along with a given trajectory. Specifically, the trajectory of the moving platform is given as  $\gamma=\beta=\alpha=0$ ,  $\mathbf{p} = [0 \ 0 \ -500 + 50 \sin t]^T \text{ mm}$ .

The input forces  $\boldsymbol{\tau}$  for the six linear actuators are calculated as functions of time  $t$ . The simulation result is plotted in Fig.3 (a), which shows that the six input forces coincide into a curve, i.e. they are equal to each other. This significance verifies the theoretical results due to the symmetrical arrangement of the six actuators.



(a) Constant orientation and variable position (b) Constant position and variable orientation

**Fig. 3.** Simulation results of the specific trajectories

For the second scenario, the trajectory of the moving platform is given as follows: the orientation of the moving platform varies by the rotation about the  $z$ -axis with a sinusoidal trajectory while the position remains constant. Specifically, the trajectory is specified as  $\gamma=\beta=0$ ,  $\alpha = \sin t$ ,  $\mathbf{p} = [0 \ 0 \ -400]^T \text{ mm}$ .

The results are plotted in Fig.3 (b) and similar to the first scenario, due to the symmetrical geometry, the input forces at actuators 1, 3 and 5 are equal to each other, and those at actuators 2, 4 and 6 are also equal to one another.

## 6 Conclusion

In this paper, a new 6-PSS parallel manipulator is investigated in 3D virtual environment and the kinematic model is built up. The inverse dynamic analysis for this parallel manipulator is performed based on the principle of virtual work. Based on the simulation results, the control strategies will be conducted for this parallel manipulator in our future research.

The implementation of the principle of virtual work leads to eliminating the constrained force at the outset. This makes it become more efficient than the conventional Newton-Euler approach on the dynamic analysis on this parallel manipulator. And the methodology of the link Jacobian matrices deduction is easy to understand, which can be also applied to the other types of parallel manipulators.

**Acknowledgments.** This work was supported in part by Macao Science and Technology Development Fund (108/2012/A3, 110/2013/A3), Research Committee of University of Macau (MYRG183(Y1-L3)FST11-LYM, MYRG203(Y1-L4)-FST11-LYM).

## References

1. Yun, Y., Li, Y.M.: Design and Analysis of a Novel 6-DOF Redundant Actuated Parallel Robot with Compliant Hinges for High Precision Positioning. *Nonlinear Dynamics* 61(4), 829–845 (2010)
2. Tsai, L.W.: Solving the Inverse Dynamics of a Stewart-Gough Manipulator by the Principle of Virtual Work. *ASME Journal of Mechanical Design* 122, 3–9 (2000)
3. Yun, Y., Li, Y.M.: A General Dynamics and Control Model of a Class of Multi-DOF Manipulators for Active Vibration Control. *Mechanism and Machine Theory* 46(10), 1549–1574 (2011)
4. Li, Y.M., Staicu, S.: Inverse Dynamics of a 3-PRC Parallel Kinematic Machine. *Nonlinear Dynamics* 67(2), 1031–1041 (2012)
5. Dasgupta, B., Choudhury, P.: A General Strategy Based on the Newton Euler Approach for the Dynamic Formulation of Parallel Manipulators. *Mechanism and Machine Theory* 34, 801–824 (1999)
6. Li, K.Q., Wen, R.: Closed-Form Dynamic Equations of the 6-RSS Parallel Mechanism Through the Newton-Euler Approach. In: *Proceedings of the Third International Conference on Measuring Technology and Mechatronics Automation*, vol. 01, pp. 712–715 (2011)
7. Harib, K., Srinivasan, K.: Kinematic and Dynamic Analysis of Stewart Platform-Based Machine Tool Structures. *Robotica* 21, 541–554 (2003)
8. Nakamura, Y., Yamane, K.: Dynamics Computation of Structure-Varying Kinematic Chains and Its Application to Human Figures. *IEEE Transactions on Robotics and Automation* 16(2), 124–134 (2000)
9. Pang, H., Shahingpoor, M.: Inverse Dynamics of a Parallel Manipulator. *Journal of Robotic System* 11(8), 693–702 (1994)
10. Penda, H., Vakil, M., Zohoor, H.: Efficient Dynamic Equation of 3-PRS Parallel Manipulator Through Lagrange Method. In: *Proceedings of the IEEE Conference on Robotics, Automation and Mechatronics*, vol. 2, pp. 1152–1157 (2004)
11. Wang, J.G., Gosselin, C.M.: A New Approach for the Dynamic Analysis of Parallel Manipulator. *Multibody System Dynamics* 2, 317–334 (1998)
12. Wang, Y.B., Zheng, S.T., Jin, J.: Dynamic Modeling of Spatial 6-DOF Parallel Manipulator Using Kane Method. In: *International Conference on E-product E-service and E-entertainment*, pp. 1–5 (2010)
13. Yun, Y., Li, Y.M.: A General Model of a Kind of Parallel Manipulator for Active Control based on Kane's Dynamics. In: *IEEE Asia Pacific Conference on Circuits and Systems*, Macao, China, pp. 1830–1833 (2008)
14. Liu, M.J., Li, C.X., Li, C.N.: Dynamics Analysis of the Gough-Stewart Platform Manipulator. *IEEE Transactions on Robotics and Automation* 16(1), 94–98 (2000)
15. Lee, K.M., Shah, D.K.: Dynamic Analysis of a Three-Degree-of-Freedom in Parallel Actuated Manipulator. *IEEE Journal of Robotics and Automation* 4(3), 361–367 (1988)
16. Lu, S., Li, Y.M.: Dimensional Synthesis of a 3-DOF Translational Parallel Manipulator Considering Kinematic Dexterity Property. In: *IEEE International Conference on Information and Automation*, Hailar, China, pp. 7–12 (2014)
17. Xu, W.Y., Li, Y.M., Xiao, X.: Kinematics and Workspace analysis for a novel 6-PSS parallel manipulator. In: *IEEE International Conference on Robotics and Biomimetics*, pp. 1869–1874 (2013)